

# Fluxional Rhenium(I) Tricarbonyl Halide Complexes of Pyrazolylpyridine Ligands. A Detailed Nuclear Magnetic Resonance Investigation

Edward W. Abel, Kevin A. Hylands, Matthew D. Olsen, Keith G. Orrell,\* Anthony G. Osborne, Vladimir Šik and Gary N. Ward

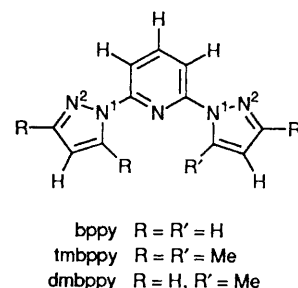
Department of Chemistry, The University, Exeter EX4 4QD, UK

2,6-Bis(pyrazol-1-yl)pyridine (bppy) reacted with pentacarbonylhalogenorhenium(I) complexes under mild conditions to form stable octahedral complexes of type *fac*-[ReX(CO)<sub>3</sub>(bppy)] (X = Cl, Br or I) in which bppy acts as a bidentate chelate ligand. In solution these tricarbonyl complexes are fluxional with bppy oscillating between equivalent bidentate bonding modes by a twist mechanism involving the breaking/making of two Re–N bonds. 2,6-Bis(3,5-dimethylpyrazol-1-yl)pyridine (tmbppy) and 2-(3,5-dimethylpyrazol-1-yl)-6-(pyrazol-1-yl)pyridine (dmbppy) formed analogous fluxional complexes. The 1,4-Re–N metallotropic shifts of [ReX(CO)<sub>3</sub>(dmbppy)] interconvert chemically distinct complexes with different solution populations. Under more severe reaction conditions the complex *cis*-[ReBr(CO)<sub>2</sub>(tmbppy)] was formed in which the ligand adopts its more usual terdentate behaviour. Rates and activation energies of these 'tick-tock' twist fluxions have been investigated by one- and two-dimensional NMR methods. Activation energies are dependent on the relative donor strengths of the N atoms, with magnitudes of  $\Delta G^\ddagger$  (298.15 K) being 55–56 (bppy),  $\approx 69$  (dmbppy) and 70–77 kJ mol<sup>-1</sup> (tmbppy).

Planar N<sub>3</sub> compounds such as 2,2':6',2''-terpyridine (terpy) usually bind to metals in a terdentate fashion if a meridional co-ordination geometry is available.<sup>1</sup> If such a geometry is not possible bidentate chelate bonding may occur leaving one of the outer pyridyl rings unco-ordinated. Recently this has been demonstrated in complexes of ruthenium(II),<sup>2,3</sup> rhenium(I)<sup>4–7</sup> and platinum(IV).<sup>5,8</sup> It is well known that the transition-metal moieties PtXMe<sub>3</sub> and ReX(CO)<sub>3</sub> (X = halide) almost invariably adopt facial configurations and so, not surprisingly, the terpy ligand is forced to act as a bidentate chelate in the octahedral complexes *fac*-[PtXMe<sub>3</sub>(terpy)] and *fac*-[ReX(CO)<sub>3</sub>(terpy)]. In such species, however, the ligand attempts to involve all three of its N atoms in metal bonding by undergoing a novel linkage-isomerization reaction.<sup>5,6</sup> Detailed NMR studies<sup>7,8</sup> have shown that the fluxion involves a twist of the metal moiety through the N–M–N angle of the octahedral centre causing a breaking and making of a pair of M–N bonds.

We have been prompted to investigate the generality of this novel type of 1,4-M–N fluxional shift in metal complexes of other N-heteroaromatic ligands. We report here our findings on ReX(CO)<sub>3</sub> complexes of the terpyridine analogue 2,6-bis(pyrazol-1-yl)pyridine (bppy) and its methyl derivatives 2,6-bis(3,5-dimethylpyrazol-1-yl)pyridine (tmbppy) and 2-(3,5-dimethylpyrazol-1-yl)-6-(pyrazol-1-yl)pyridine (dmbppy). These compounds were chosen for a variety of reasons. There is considerable interest in the photochemical, photophysical and redox properties of ruthenium complexes of these<sup>9</sup> and related<sup>10–12</sup> pyrazolylpyridines a convenient synthetic route to them has recently been described<sup>13</sup> and the crystal structure of bppy has lately been reported.<sup>14</sup>

Variable temperature one- and two-dimensional NMR studies of the solution fluxionality of the complexes *fac*-[ReX(CO)<sub>3</sub>L] (L = bppy or tmbppy, X = Cl, Br or I; L = dmbppy, X = Br) will now be presented. We also report <sup>1</sup>H NMR data for the complex *cis*-[ReBr(CO)<sub>2</sub>(tmbppy)] formed from the tricarbonyl complex under more forcing reaction conditions. This complex is non-fluxional, with the ligand adopting its more usual terdentate bonding mode.



## Experimental

**Materials.**—The compounds [ReX(CO)<sub>5</sub>] (X = Cl, Br or I) were prepared by previous methods;<sup>15,16</sup> bppy and its methyl derivatives, tmbppy and dmbppy, were prepared by the recent method of Jameson and Goldsby.<sup>13</sup>

**Synthesis of Complexes.**—All preparations were performed by standard Schlenk techniques<sup>17</sup> under purified nitrogen using freshly distilled, dried and degassed solvents. The complexes [ReX(CO)<sub>3</sub>L] (L = bppy or tmbppy, X = Cl, Br or I; L = dmbppy, X = Br) were all prepared in an analogous manner, synthetic data being given in Table 1. The preparation of [ReBr(CO)<sub>3</sub>(tmbppy)] is given as a representative example.

[2,6-Bis(3,5-dimethylpyrazol-1-yl)pyridine]bromotricarbonylrhenium(I). The compound [ReBr(CO)<sub>3</sub>] (0.10 g, 0.25 mmol) and tmbppy (0.10 g, 0.38 mmol) were dissolved in benzene (25 cm<sup>3</sup>) with stirring and gentle warming to give a colourless solution. On heating for 1 h the solution became lime-yellow. Light petroleum (b.p. 60–80 °C, 50 cm<sup>3</sup>) was added and the mixture heated under reflux for 4 h. After cooling overnight a yellow crystalline product was precipitated. The pale yellow benzene–light petroleum mixture was decanted off. The solid was washed *in situ* with diethyl ether (2 × 40 cm<sup>3</sup>) and then

**Table 1** Synthetic and analytical data for the complexes [ReX(CO)<sub>3</sub>L] (L = bppy or tmbppy; X = Cl, Br or I), [ReBr(CO)<sub>3</sub>(dmbppy)] and [ReBr(CO)<sub>2</sub>(tmbppy)]

Complex	M.p. <sup>a</sup> /°C	Yield <sup>b</sup> (%)	$\tilde{\nu}_{\text{CO}}$ <sup>c</sup> /cm <sup>-1</sup>	Analysis <sup>d</sup> (%)		
				C	H	N
[ReCl(CO) <sub>3</sub> (bppy)]	251–252	75	2025vs, 1940s, 1908s	32.9 (32.5)	1.9 (1.7)	12.9 (13.6)
[ReBr(CO) <sub>3</sub> (bppy)]	219–221	87	2037vs, 1942s, 1912s	29.8 (29.9)	1.4 (1.6)	12.2 (12.5)
[ReI(CO) <sub>3</sub> (bppy)]	249–250	98	2030vs, 1945s, 1912s	28.0 (27.6)	1.4 (1.5)	11.6 (11.5)
[ReCl(CO) <sub>3</sub> (tmbppy)]	259–260	85	2022vs, 1932s, 1908s	34.4 (34.7) <sup>e</sup>	2.7 (2.9) <sup>e</sup>	10.4 (10.7) <sup>e</sup>
[ReBr(CO) <sub>3</sub> (tmbppy)]	265–266	96	2032vs, 1933s, 1907s	35.4 (35.0)	2.7 (2.8)	11.1 (11.3)
[ReI(CO) <sub>3</sub> (tmbppy)]	245–247	82	2020vs, 1935s, 1908s	32.8 (32.5)	2.6 (2.6)	10.5 (10.5)
[ReBr(CO) <sub>3</sub> (dmbppy)]	272–275	96	2035vs, 1937s, 1910s	32.8 (32.7)	2.1 (2.2)	11.7 (11.9)
[ReBr(CO) <sub>2</sub> (tmbppy)]	> 355	23	1892s, <sup>f</sup> 1829s <sup>f</sup>	35.0 (34.6)	2.7 (2.9)	11.7 (11.9)

<sup>a</sup> With decomposition. <sup>b</sup> Yield quoted relative to metal-containing reactant. <sup>c</sup> Recorded in CHCl<sub>3</sub> solution; s = strong, v = very. <sup>d</sup> Calculated values in parentheses. <sup>e</sup> Figures allow for inclusion of solvent of crystallisation, *i.e.* [ReCl(CO)<sub>3</sub>(tmbppy)]·CH<sub>2</sub>Cl<sub>2</sub>. <sup>f</sup> Recorded as a KBr disc.

dried under vacuum to give yellow crystals. Yield 0.146 g (96%).

The terdentate ligand complex [ReBr(CO)<sub>2</sub>(tmbppy)] was prepared as follows.

[2,6-Bis(3,5-dimethylpyrazol-1-yl)pyridine]bromodicarbonyl-rhenium(I). The complex [ReBr(CO)<sub>3</sub>(tmbppy)] (0.1 g, 0.16 mmol) was sealed in an evacuated glass Carius tube and placed in an oven at 270 °C for 5 h. After cooling, the black solid was removed from the tube and stirred with chloroform (15 cm<sup>3</sup>) for *ca.* 30 h. The pale yellow supernatant liquid was decanted, the black solid washed with diethyl ether (10 cm<sup>3</sup>) and then dried *in vacuo*. Yield 0.022 g (23%).

**Physical Methods.**—Hydrogen-1 and carbon-13 NMR spectra were recorded on Bruker AM250 or ACF300 spectrometers operating respectively at 250.13 and 300.13 MHz for <sup>1</sup>H, and 62.90 and 75.47 MHz for <sup>13</sup>C. Spectra were recorded of CDCl<sub>3</sub>, CD<sub>2</sub>Cl<sub>2</sub> or CDCl<sub>2</sub>CDCl<sub>2</sub> solutions of the complexes, with SiMe<sub>4</sub> as an internal standard. Standard B-VT1000 variable-temperature units were used to control the probe temperatures. Temperatures, based on calibration against a Comark digital thermometer, are considered accurate to ±1 °C. The <sup>13</sup>C–<sup>1</sup>H correlation spectra of [ReI(CO)<sub>3</sub>(tmbppy)] were based on the Bruker automation programs XHCCORR.AU for one-bond correlations measured in direct mode and INVDR2LP.AU for longer-range correlations measured in inverse mode. The delay parameter *D*4 for the two programs was chosen as 0.001 65 s ( $\equiv J = 151.5$  Hz) and 0.05 s ( $\equiv J = 10$  Hz) respectively. The <sup>1</sup>H two-dimensional correlation (COSY) and exchange (EXSY) spectra recorded for [ReBr(CO)<sub>3</sub>(dmbppy)] used the standard Bruker automation programs COSY.AU and NOESYPH.AU respectively. The relaxation delay was 2 s and the evolution time had an initial value of  $3 \times 10^{-6}$  s. In the two-dimensional EXSY experiment a mixing time of 0.5 s was used. Data processing incorporated a sine-bell window function (COSY) or exponential function (line broadening 0.5 Hz). Kinetic data were derived from total bandshape analyses of <sup>1</sup>H NMR spectra using the authors' version of the standard DNMR program.<sup>18</sup>

Infrared spectra of CHCl<sub>3</sub> solutions of the complexes were recorded on a Perkin Elmer 881 spectrometer, calibrated from the line of polystyrene at 1602 cm<sup>-1</sup>.

Elemental analyses (C, H and N) were carried out by Butterworth Laboratories Ltd., Teddington, Middlesex, London.

## Results

High yields of the complexes [ReX(CO)<sub>3</sub>L] (L = bppy or tmbppy, X = Cl, Br or I) as air-stable, yellow crystalline solids were obtained. In CHCl<sub>3</sub> solution all complexes displayed three strong carbonyl stretching bands in the infrared (Table 1) indicative of *fac* stereochemistry, and implying that the bppy ligands were acting as bidentate chelates. This was confirmed by solution NMR spectroscopy (see later). Heating a sample of [ReBr(CO)<sub>3</sub>(tmbppy)] in a sealed, evacuated glass Carius tube produced a black solid which was only sparingly soluble in organic solvents. This compound was identified as *cis*-[ReBr(CO)<sub>2</sub>(tmbppy)] on the basis of analytical and IR data (two carbonyl bands at appreciably lower wavenumbers than for the tricarbonyl complexes), and a simpler <sup>1</sup>H NMR spectrum (see later) indicative of a terdentate 3N ligand.

**Static NMR Studies.**—(i) *Free pyrazolylpyridines.* Chemical shift data for all three compounds are given in Table 2 where it will be observed that  $\delta_{\text{C/F}} > \delta_{\text{A/D}}$  for both ring and methyl hydrogens. This presumably arises from the preferred *trans*, *trans* configuration of the rings, a configuration known to exist in the solid state,<sup>14</sup> and which leads to a relative deshielding of the 'inner' hydrogens or methyls C and F compared to the 'outer' pair A and D. Strong evidence for such a configuration in solution comes from the <sup>1</sup>H NMR spectrum of dmbppy where a strong nuclear Overhauser effect (NOE) between H<sub>C</sub> and Me<sub>F</sub> was detected in an NOE difference experiment [Fig. 1(a)]. No such NOE was detected between H<sub>C</sub> and Me<sub>D</sub> [Fig. 1(b)].

(ii) [ReX(CO)<sub>3</sub>(bppy)] *Complexes.* Hydrogen-1 chemical shifts ( $\delta$ ) and co-ordination shifts ( $\Delta\delta$ ) are recorded in Table 3 for all three complexes (X = Cl, Br or I). In all cases, significant high-frequency co-ordination shifts occur at the A and B positions,  $\Delta\delta_{\text{A}} \approx 0.43$ ,  $\Delta\delta_{\text{B}} \approx 0.33$ , and small low-frequency shifts at H<sub>C</sub>,  $\Delta\delta_{\text{C}} \approx -0.13$ . Smaller high-frequency shifts occur at the D and E positions of the unco-ordinated pyrazole ring as expected but the hydrogen H<sub>F</sub> experiences a large low-frequency shift ( $\Delta\delta_{\text{F}} \approx -0.4$ , X = Br or I) due to the 180° rotation of the unco-ordinated pyrazole ring which is required to produce the *cis*, *cis* configuration of the ligand rings in the rhenium complexes. The appreciably smaller co-ordination shift  $\Delta\delta_{\text{F}}$  of  $-0.17$  in the X = Cl complex is attributed to a specific solute-solvent interaction. The hydrogen in position H exhibits a large low-frequency shift which is probably the result of H<sub>H</sub>–H<sub>F</sub>

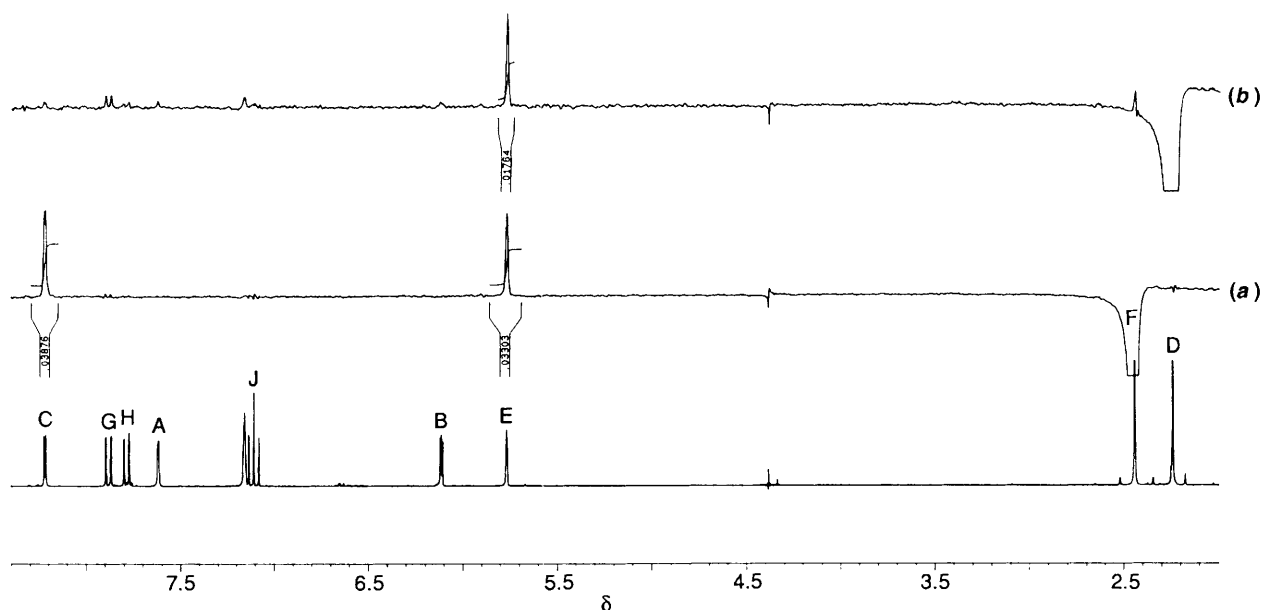
**Table 2** Hydrogen-1 NMR data<sup>a</sup> for the pyrazolylpyridine ligands at 303 K

	Solvent	$\delta_A$	$\delta_B$	$\delta_C$	$\delta_D$	$\delta_E$	$\delta_F$	$\delta_G$	$\delta_H$	$\delta_I$
bppy	CDCl <sub>3</sub>	7.76	6.50	8.57	7.76	6.50	8.57	7.86	7.86	7.93
tmbppy	CDCl <sub>3</sub>	2.30	6.00	2.59	2.30	6.00	2.59	7.69	7.69	7.88
	(CD <sub>3</sub> ) <sub>2</sub> SO	2.21	6.14	2.55	2.21	6.14	2.55	7.68	7.68	8.06
dmbppy	CDCl <sub>3</sub>	7.75	6.48	8.44 <sup>b</sup>	2.31	6.04	2.75 <sup>b</sup>	7.82	7.78	7.90

	Solvent	$J_{AB}$	$J_{AC}$	$J_{BC}$	$J_{GJ}$	$J_{HJ}$	$J_{DE}$	$J_{DF}$	$J_{EF}$	$J_{GH}$
bppy	CDCl <sub>3</sub>	1.6	0.6	2.6	8.13	8.13	1.6	0.6	2.6	?
tmbppy	CDCl <sub>3</sub>	≈ 0	≈ 0	0.65	8.2	8.2	≈ 0	≈ 0	0.65	?
dmbppy	CDCl <sub>3</sub>	1.6	0.7	2.6	8.1	8.1	≈ 0	≈ 0	0.7	0.9

<sup>a</sup> Chemical shifts relative to SiMe<sub>4</sub>,  $\delta$  0; scalar couplings  $J_{ij}$  in Hz. <sup>b</sup> Large NOE interaction, see Fig. 1(a).



**Fig. 1** The 250 MHz <sup>1</sup>H NMR spectrum of dmbppy in C<sub>6</sub>D<sub>6</sub> and two NOE difference experiments involving irradiation at (a) Me<sub>F</sub> and (b) Me<sub>D</sub>. The strong positive NOE of H<sub>c</sub> in (a) confirms the *trans, trans* conformation of the ligand

shielding in the complex compared to H<sub>H</sub>-N<sup>2</sup> deshielding in the free pyrazolylpyridine. Finally, the hydrogen H<sub>J</sub> on the pyridyl ring experiences a large high-frequency shift on co-ordination.

The scalar coupling constants,  $J_{AB}$  and  $J_{BC}$  increase significantly (by ≈ 0.6 Hz) on co-ordination whereas  $J_{GJ}$  and  $J_{HJ}$  respectively increase and decrease by smaller amounts. The couplings  $J_{BC}$ ,  $J_{GJ}$  and  $J_{HJ}$  appear to be slightly halogen dependent such that I > Br > Cl ( $J_{BC}$ ,  $J_{GJ}$ ) and Cl > Br > I ( $J_{HJ}$ ).

(iii) [ReX(CO)<sub>3</sub>(tmbppy)]. Hydrogen-1 chemical shifts, co-ordination shifts and H-H scalar couplings of all three halide complexes are given in Table 4. Certain co-ordination shifts showed analogous trends to those of the bppy complexes. Thus, substantial high-frequency co-ordination shifts occurred to Me<sub>A</sub>, H<sub>B</sub> and H<sub>J</sub>, with a smaller shift in the same direction at Me<sub>C</sub>. The hydrogens Me<sub>F</sub> and H<sub>H</sub> experience sizeable low-

frequency shifts (with  $|\Delta\delta_{HI}| \gg |\Delta\delta_{FI}|$ ) again due to the 180° rotation of the unco-ordinated pyrazole ring relative to the free pyrazolylpyridine configuration.

In these complexes no significant changes in the  $J_{HH}$  couplings were found.

Carbon-13 chemical shifts of tmbppy and its complex [ReI(CO)<sub>3</sub>(tmbppy)] are given in Table 5. Correlations of the <sup>13</sup>C and <sup>1</sup>H shifts of this complex were derived from the two-dimensional correlation spectra shown in Figs. 2 and 3 which respectively identify one-bond and longer-range (two- and/or three-bond) <sup>13</sup>C-<sup>1</sup>H correlations. In order to aid <sup>13</sup>C NMR detection of the carbonyl signals of this complex some relaxation reagent [Cr(acac)<sub>3</sub>] (acac = acetylacetonate) was added to the solution. When the <sup>1</sup>H NMR spectrum of this solution was examined the signals due to hydrogens H<sub>G</sub>, H<sub>J</sub> and Me<sub>C</sub> were notably broadened with respect to the remainder,

**Table 3** Hydrogen-1 NMR data<sup>a</sup> for the complexes [ReX(CO)<sub>3</sub>(bppy)] at 223 K

X	Solvent Co-ordination shift	δ <sub>A</sub>	δ <sub>B</sub>	δ <sub>C</sub>	δ <sub>D</sub>	δ <sub>E</sub>	δ <sub>F</sub>	δ <sub>G</sub>	δ <sub>H</sub>	δ <sub>I</sub>
		I	CDCl <sub>3</sub>	8.22	6.85	8.44	7.97	6.68	8.15	7.87
Br	CD <sub>2</sub> Cl <sub>2</sub>	0.46	0.35	-0.13	0.21	0.18	-0.42	0.01	-0.38	0.34
	Δδ <sup>b</sup>	8.17	6.80	8.42	7.91	6.66	8.17	7.82	7.48	8.24
Cl	CDCl <sub>3</sub>	0.41	0.30	-0.15	0.15	0.16	-0.40	-0.04	-0.21	0.36
	Δδ <sup>b</sup>	8.20	6.83	8.45	7.96	6.68	8.40	7.82	7.56	8.26
		0.44	0.33	-0.12	0.20	0.18	-0.17	-0.04	-0.30	0.33
		<sup>3</sup> J <sub>AB</sub>	<sup>4</sup> J <sub>AC</sub>	<sup>3</sup> J <sub>BC</sub>	<sup>3</sup> J <sub>GJ</sub>	<sup>3</sup> J <sub>HJ</sub>	<sup>3</sup> J <sub>DE</sub>	<sup>4</sup> J <sub>DF</sub>	<sup>3</sup> J <sub>EF</sub>	<sup>4</sup> J <sub>GH</sub>
I	CDCl <sub>3</sub>	2.0	≈0	3.0	8.3	7.6	1.6	≈0	2.5	0.7
Br	CD <sub>2</sub> Cl <sub>2</sub>	2.2	≈0	2.9	8.3	7.9	1.4	≈0	2.2	0.8
Cl	CDCl <sub>3</sub>	2.2	≈0	2.5	8.1	8.0	1.7	≈0	2.9	≈0.7

<sup>a</sup> Chemical shifts relative to internal SiMe<sub>4</sub>, δ 0; scalar couplings  $J_{ij}$  in Hz. <sup>b</sup> Co-ordination shifts (*i.e.* relative to bppy).

**Table 4** Hydrogen-1 NMR data<sup>a</sup> for the complexes [ReX(CO)<sub>3</sub>(tmbppy)] at 303 K

X	Solvent Co-ordination shift	δ <sub>A</sub>	δ <sub>B</sub>	δ <sub>C</sub>	δ <sub>D</sub>	δ <sub>E</sub>	δ <sub>F</sub>	δ <sub>G</sub>	δ <sub>H</sub>	δ <sub>I</sub>
		I	CDCl <sub>3</sub>	2.62	6.29	2.76	2.32	6.15	2.44	7.73
Br	CDCl <sub>3</sub>	0.32	0.29	0.17	0.02	0.15	-0.15	0.04	-0.50	0.22
	Δδ <sup>b</sup>	2.62	6.28	2.74	2.32	6.15	2.40	7.74	7.20	8.10
Cl	CDCl <sub>3</sub>	0.32	0.28	0.15	0.02	0.15	-0.19	0.05	-0.49	0.22
	CD <sub>2</sub> Cl <sub>2</sub>	2.61	6.33	2.75	2.29	6.14	2.34	7.80	7.22	8.15
	Δδ <sup>b</sup>	0.31	0.33	0.16	-0.01	0.14	-0.15	0.11	-0.47	0.27
		<sup>4</sup> J <sub>AB</sub>	<sup>6</sup> J <sub>AC</sub>	<sup>4</sup> J <sub>BC</sub>	<sup>3</sup> J <sub>GJ</sub>	<sup>3</sup> J <sub>HJ</sub>	<sup>4</sup> J <sub>DE</sub>	<sup>6</sup> J <sub>DF</sub>	<sup>4</sup> J <sub>EF</sub>	<sup>4</sup> J <sub>GH</sub>
I	CDCl <sub>3</sub>	≈0	≈0	≈0.7	8.0	8.0	≈0	≈0	≈0.7	0.8
Br	CDCl <sub>3</sub>	≈0	≈0	≈0.7	8.0	8.0	≈0	≈0	≈0.7	≈1
Cl	CD <sub>2</sub> Cl <sub>2</sub>	≈0	≈0	≈0.7	8.1	8.1	≈0	≈0	≈0.7	≈1

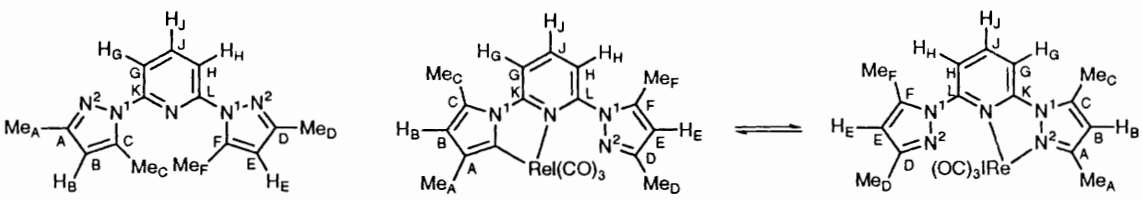
<sup>a</sup> Shifts relative to internal SiMe<sub>4</sub>, δ 0; scalar couplings  $J_{ij}$  in Hz. <sup>b</sup> Co-ordination shifts (*i.e.* relative to tmbppy).

clearly due to reduction in the spin-spin relaxation times,  $T_2$ , of these nuclei. This suggests that the rhenium(I) complex preferentially binds to [Cr(acac)<sub>3</sub>] via the lone pair of the nitrogen (N<sup>1</sup>) of the five-membered chelate ring. This is not unexpected in view of the rotational effects of the uncoordinated pyrazole ring which will hinder close approach of the [Cr(acac)<sub>3</sub>] molecule to the corresponding nitrogen of that ring.

Many of the trends in the <sup>13</sup>C co-ordination shifts mirrored those in the <sup>1</sup>H shifts but were greater in magnitude. For example, large high-frequency shifts occurred at the A and B position carbons ( $\Delta\delta_A = 5.59$ ,  $\Delta\delta_B = 4.54$ ), and a somewhat smaller shift at the C position ( $\Delta\delta_C = 2.06$ ). Notably the carbon at the G position of the pyridyl ring experiences a low-frequency

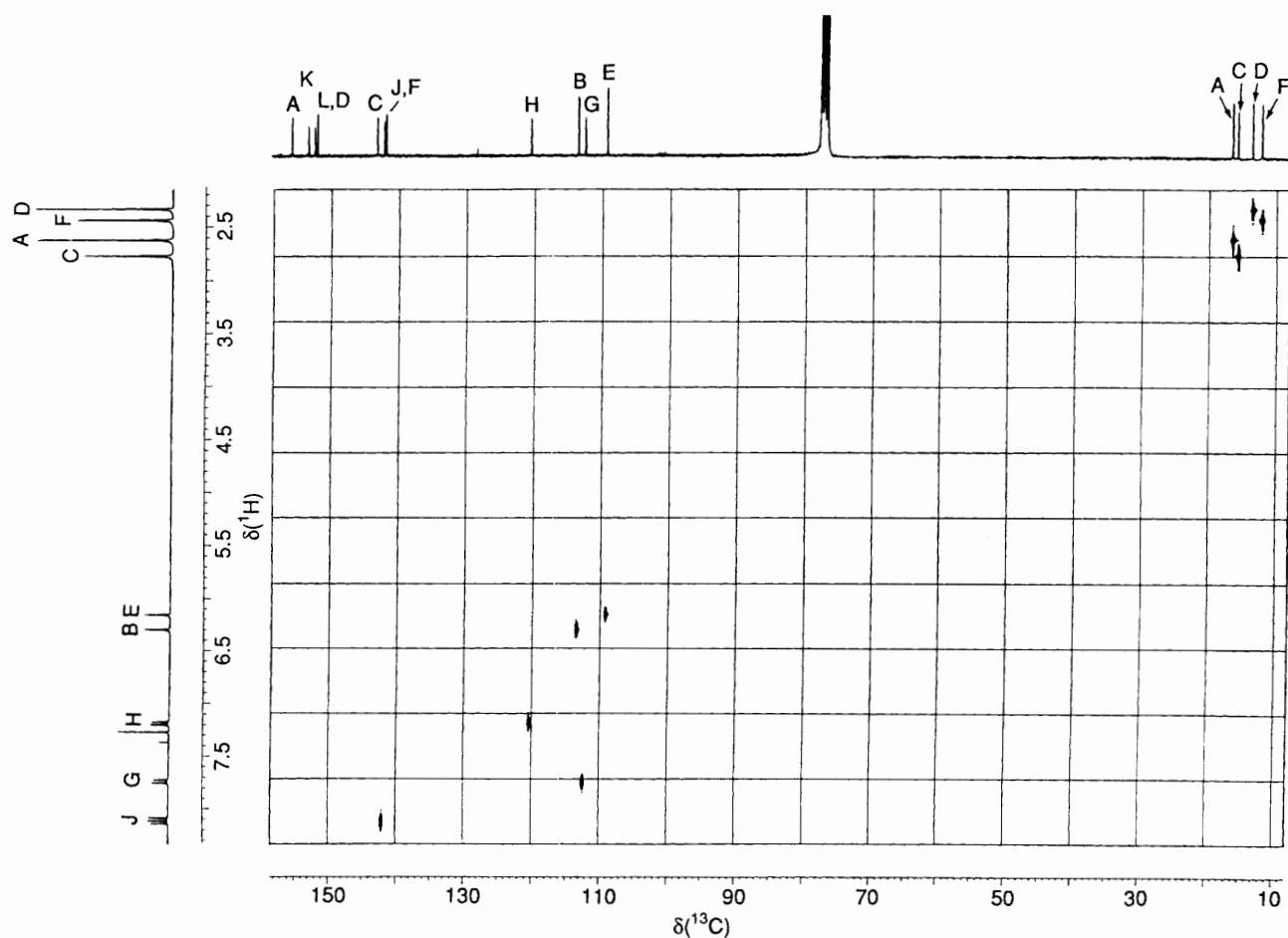
shift, whereas that at H exhibits a large high-frequency shift. The carbon of Me<sub>F</sub> experiences a sizeable low-frequency shift probably as a result of the rotation of this ring on co-ordination. The methyl carbons of Me<sub>A</sub> and Me<sub>C</sub> show high-frequency shifts in contrast to Me<sub>D</sub> and Me<sub>F</sub>. It is particularly noteworthy that the co-ordination shifts of C<sub>H</sub> (Table 5) and H<sub>H</sub> (Table 4) are greatest in magnitude but of opposite signs! This probably reflects the anisotropic shielding effects of the uncoordinated pyrazole ring arising from the different rotational conformers of the ring in the free pyrazolylpyridine and in the complexes.

A more detailed rationalization of these co-ordination shifts is not straightforward and probably not a fruitful exercise. Ligand-to-metal  $\sigma$  donation, metal-to-ligand  $\pi$  back donation,

**Table 5** Carbon-13 NMR chemical shift data<sup>a</sup> for tmbppy and [ReI(CO)<sub>3</sub>(tmbppy)] at 303 K in CDCl<sub>3</sub>


Compound	$\delta_A$	$\delta_B$	$\delta_C$	$\delta_D$	$\delta_E$	$\delta_F$	$\delta_G$	$\delta_H$	$\delta_I$	$\delta_J$	$\delta_K$	$\delta_L$	$\delta_{Me_A}$	$\delta_{Me_C}$	$\delta_{Me_D}$	$\delta_{Me_F}$
tmbppy	150.07	108.91	141.02	150.07	108.91	141.02	113.69	113.69	140.37	151.49	151.49	13.58	14.04	13.58	14.04	
[ReI(CO) <sub>3</sub> (tmbppy)] <sup>b</sup>	155.66	113.45	143.08	151.91	109.20	141.77	112.43	120.38	142.02	153.23 <sup>c</sup>	152.28 <sup>c</sup>	16.43	15.62	13.46	12.06	
$\Delta\delta^d$	5.59	4.54	2.06	1.84	0.29	0.75	-1.26	6.69	1.65	1.74	0.79	2.85	1.58	-0.12	-1.98	

<sup>a</sup> Relative to internal SiMe<sub>4</sub>;  $\delta$  0. <sup>b</sup> Additional CO shifts at  $\delta$  195.33 (equatorial), 191.77 (equatorial) and 188.64 (axial) using [Cr(acac)<sub>3</sub>]. See Fig. 9. <sup>c</sup> Assignments possibly reversed. <sup>d</sup> Co-ordination shift (*i.e.* relative to tmbppy).

**Fig. 2** The <sup>1</sup>H-<sup>13</sup>C NMR correlation spectrum (one-bond correlations only) of [ReI(CO)<sub>3</sub>(tmbppy)] in CDCl<sub>3</sub> at room temperature

chelation-imposed conformational changes, co-ordinative disruption of interring conjugation and even interligand ring-current anisotropy effects have all been invoked previously<sup>10</sup> to explain co-ordination shifts in tris(ligand)ruthenium(II) complexes, and all may indeed play a role in determining the shifts in the present rhenium(I) complexes, but their relative contributions are almost impossible to assess.

The one-, two-, and three-bond C-H scalar couplings for tmbppy and the complex [ReI(CO)<sub>3</sub>(tmbppy)] are given in Table 6. These were measured by a combination of proton-

coupled one-dimensional <sup>13</sup>C NMR and two-dimensional <sup>13</sup>C-<sup>1</sup>H heteronuclear multiple bond correlation (HMBC) NMR spectroscopy (Fig. 3). The well established trend<sup>19</sup> in aromatic systems that <sup>1</sup>J<sub>CH</sub> ≫ <sup>3</sup>J<sub>CCH} > <sup>2</sup>J<sub>CCH} is followed in the five- and six-membered N-heterocyclic rings of these pyrazolopyridines. One-bond couplings associated with the *co-ordinated* pyrazole ring in most cases increase considerably on co-ordination whereas analogous couplings in the other pyrazole ring are rather less affected. For example, in the case of ring CH moieties, <sup>1</sup>J<sub>CH} increases from 172.5 to 180.0 Hz when associated</sub></sub></sub>

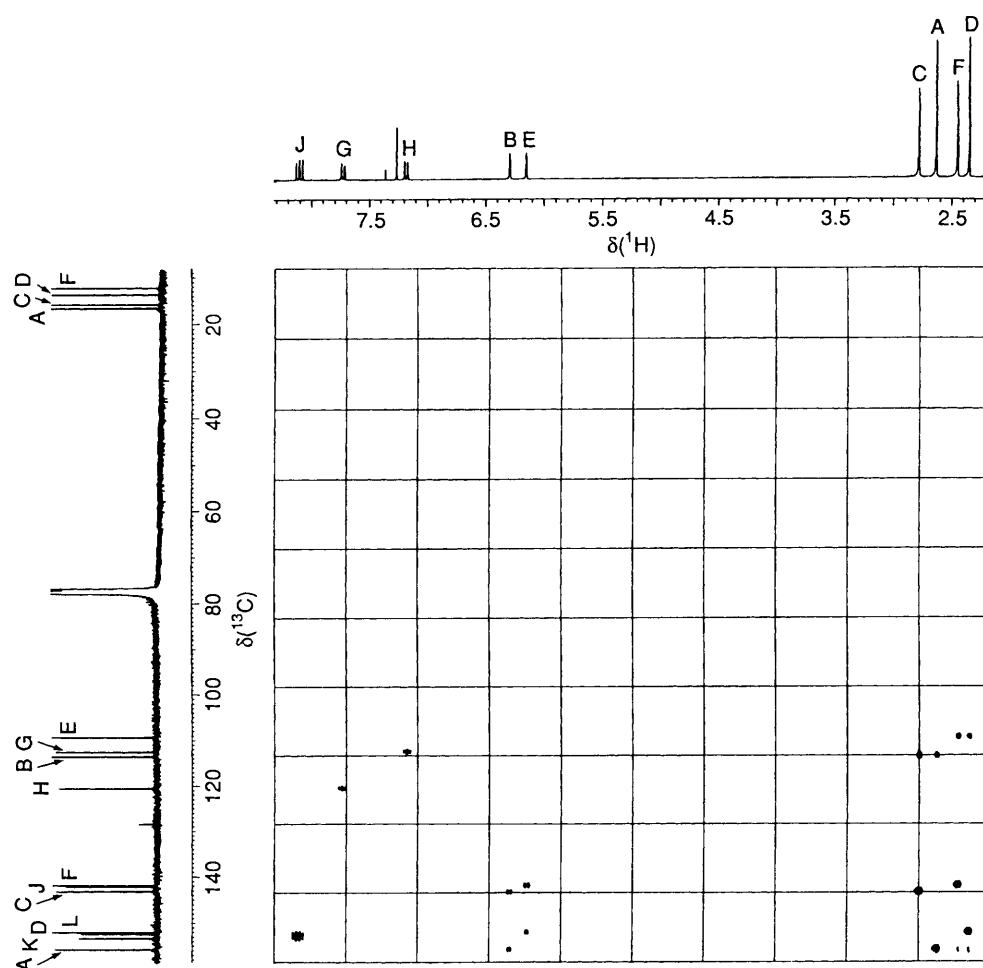


Fig. 3 Long-range (two- and/or three-bond)  $^1\text{H}$ - $^{13}\text{C}$  correlation spectrum (HMBC in inverse mode) of  $[\text{ReI}(\text{CO})_3(\text{tmbppy})]$  in  $\text{CDCl}_3$  at room temperature

Table 6 The NMR C-H scalar couplings in  $\text{tmbppy}^a$  and  $[\text{ReI}(\text{CO})_3(\text{tmbppy})]$

Carbon <sup>b</sup>	$^1J_{\text{CH}}/\text{Hz}$	$^2J_{\text{CCH}}/\text{Hz}$	$^3J_{\text{CCCH}}/\text{Hz}$	Carbon <sup>b</sup>	$^1J_{\text{CH}}/\text{Hz}$	$^2J_{\text{CCH}}/\text{Hz}$	$^3J_{\text{CCCH}}/\text{Hz}$
A	—	6.5( $\text{Me}_A$ ) ( $\approx 6$ )	—	G	170.0 (171.0)	<1	7.0( $\text{H}_H$ ) (6.8)
		6.5( $\text{H}_B$ ) ( $\approx 6$ )		H	172.0 (171.0)	<1	7.0( $\text{H}_G$ ) (6.8)
B	180.0 (172.5)	—	3.5( $\text{Me}_C$ ) (3.5)	J	168.5 (164.7)	<1	—
			3.5( $\text{Me}_A$ ) (3.5)	K	—	<1	9.5( $\text{H}_J$ ) (9.7)
C	—	$\approx 6.5(\text{Me}_C)$ (7.0)	—	L	—	<1	9.5( $\text{H}_J$ ) (9.7)
		$\approx 6.5(\text{H}_B)$ (8.8)		$\text{Me}_A$	130.0 (122.0)	—	<1
D	—	$\approx 6(\text{Me}_D)$ ( $\approx 6$ )	—	$\text{Me}_C$	130.0 (129.3)	—	1.8( $\text{H}_B$ ) (1.6)
		$\approx 6(\text{H}_E)$ ( $\approx 6$ )		$\text{Me}_D$	127.0 (122.0)	—	<1
E	174.5 (172.5)	—	$\approx 3.5(\text{Me}_D)$ (3.5)	$\text{Me}_F$	129.5 (129.3)	—	1.0( $\text{H}_E$ ) (1.6)
			3.5( $\text{Me}_F$ ) (3.5)				
F	—	9.0( $\text{H}_E$ ) (8.8)	—				
		6.5( $\text{Me}_F$ ) (7.0)					

<sup>a</sup> Values in parentheses. <sup>b</sup> See Table 5 for labelling. <sup>c</sup> Origin of hydrogen couplings shown in parentheses.

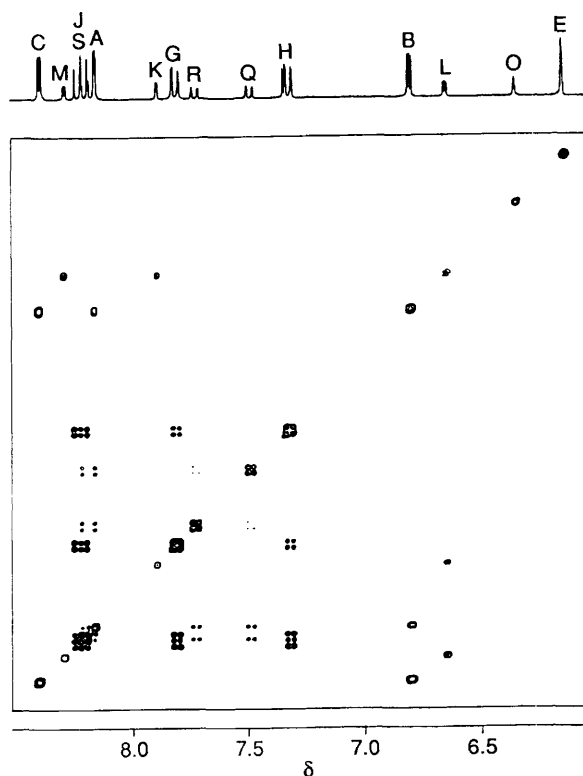


Fig. 4 The  $^1\text{H}$ - $^1\text{H}$  COSY spectrum of  $[\text{ReBr}(\text{CO})_3(\text{dmbppy})]$  in  $\text{CD}_2\text{Cl}_2$  at  $-10^\circ\text{C}$ . Aromatic region only is shown

with the co-ordinated ring (B position) but only from 172.5 to 174.5 Hz when part of the unco-ordinated ring (E position). In the case of ring methyls the increases in  $^1J_{\text{CH}}$  on co-ordination are considerably greater for the 3-position methyls  $\text{Me}_A$  and  $\text{Me}_D$  compared to the 5-position methyls  $\text{Me}_C$  and  $\text{Me}_F$ . In contrast,  $^2J_{\text{CCH}}$  values decrease somewhat on co-ordination, *viz.*  $^2J_{\text{CCH}}$  values of the C-position carbon decrease from 8.8 and 7.0 to 6.5 and 6.5 Hz on co-ordination. In the central pyridyl ring all  $^2J_{\text{CCH}}$  couplings were vanishingly small. The methyls  $\text{Me}_C$  and  $\text{Me}_F$  were distinguished from  $\text{Me}_A$  and  $\text{Me}_D$  in both the free pyrazolylpyridine and the complex by their measurable couplings to *ortho*-CH nuclei. This applies to both H-H and C-H couplings, *viz.* the H-H coupling  $^4J_{\text{BC}} = 0.7$  Hz and the C-H coupling  $^3J_{\text{BC}} = 1.8$  Hz. No comparable couplings were observed for methyls  $\text{Me}_A$  and  $\text{Me}_D$ .

(iv)  $[\text{ReBr}(\text{CO})_3(\text{dmbppy})]$ . The hydrogen-1 chemical shifts of this complex mixture were measured in  $\text{CDCl}_3$  and  $\text{CD}_2\text{Cl}_2$  solutions at ambient temperatures where the fluxional exchange was slow on the NMR chemical shift time-scale. Signals due to 14 ring and four methyl hydrogens of these two chemically different rhenium(I) complexes were detected and assigned unambiguously by two-dimensional COSY experiments and by analogy with the spectra of the corresponding bpy and tmbppy complexes. The  $^1\text{H}$  two-dimensional COSY spectrum of the complexes in  $\text{CD}_2\text{Cl}_2$  at  $-10^\circ\text{C}$  is shown in Fig. 4. The two complexes were present in an abundance ratio of 3:1, the more abundant species being the one involving co-ordination to the unsubstituted pyrazole ring. Presumably, the pyrazole ring methyls act as slight steric deterrents to co-ordination to that ring. The spectra in  $\text{CD}_2\text{Cl}_2$  and  $\text{CDCl}_3$  differ somewhat, particularly in the relative positions of the  $\text{H}_C$  and  $\text{H}_M$  signals (Table 7). The co-ordination shifts follow the predictions for the complexes of bpy and tmbppy, with the exceptions of the hydrogens at the C and M ring positions, and the methyls at the F and P positions. These are the positions most sensitive to the

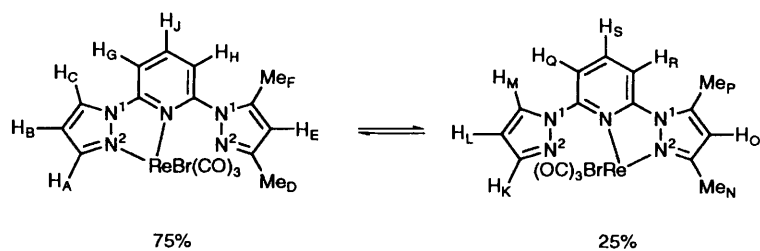
change in configuration of the pyrazole rings on co-ordination and to the rotational behaviour of the unco-ordinated pyrazole rings. The changes in scalar H-H couplings on co-ordination are fairly minor but it is noted that  $J_{\text{AB}}$ ,  $J_{\text{BC}}$  and  $J_{\text{GJ}}$  increase slightly whereas  $J_{\text{HJ}}$  decreases somewhat.

(v)  $[\text{ReBr}(\text{CO})_2(\text{tmbppy})]$ . The hydrogen-1 chemical shifts of this terdentate ligand complex are given in Table 8. The co-ordination shifts are compared with those for the bidentate complex  $[\text{ReBr}(\text{CO})_3(\text{tmbppy})]$  in both the fast- and slow-exchange regimes. Co-ordination shifts of the terdentate species are now all sizeably positive ( $\Delta\delta = 0.2 - 0.4$ ) in contrast to the bidentate ligand shifts. For hydrogens or methyls of the pyrazole ring  $\Delta\delta_B$ ,  $\Delta\delta_C$ ,  $\Delta\delta_E$  and  $\Delta\delta_F$  values are much larger than the averaged values of the bidentate complex. For the pyridyl hydrogens  $\Delta\delta_G$  and  $\Delta\delta_H$  are strongly positive in contrast to the bidentate complex, whereas  $\Delta\delta_I$  is hardly changed. All these data point towards stronger Re-N interactions in the terdentate ligand species.

*Dynamic NMR Studies.*—(i)  $[\text{ReX}(\text{CO})_3(\text{bppy})]$ . The three complexes ( $X = \text{Cl}, \text{Br}$  or  $\text{I}$ ) gave similar  $^1\text{H}$  NMR spectra at *ca.*  $-50^\circ\text{C}$  all being indicative of non-fluxional bidentate complexes. On warming the NMR solutions, however, to ambient temperatures, all spectral lines broadened, with the notable exception of the  $\text{H}_J$  signal, with pairs of lines eventually coalescing and then sharpening according to the exchange schemes  $\text{ABC} \rightleftharpoons \text{DEF}$  and  $\text{GHJ} \rightleftharpoons \text{HGJ}$ . This is clearly the result of the fluxional process involving 1,4 shifts of the pair of Re-N bonds according to the structures shown at the head of Table 3. The unique J position hydrogen of the pyridyl ring is quite unaffected by this movement as was noted in the case of the analogous terpyridine complexes.<sup>7</sup> The variable-temperature  $^1\text{H}$  NMR spectra of the  $X = \text{Cl}$  complex are shown in Fig. 5. Rates of the fluxional process were deduced by bandshape analysis of the signals of the central pyridyl ring and the 'best-fit' spectra are shown alongside the experimental spectra in Fig. 5. Rate data for the fluxions in the other complexes were extracted by similar bandshape methods. For  $X = \text{Br}$ , the exchange of the B and E signals of the  $\text{ABC} \rightleftharpoons \text{DEF}$  spin system was measured, whereas for the  $X = \text{I}$  complex the pyridyl hydrogen signals were fitted. In this case the resulting rate data were used to fit the remainder of the spectra so that true total bandshape analysis was achieved. Activation-energy data were derived from the rate data in the usual way and given in Table 9.

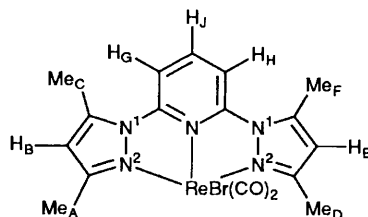
(ii)  $[\text{ReX}(\text{CO})_3(\text{tmbppy})]$ . In contrast to the bpy complexes these tmbppy complexes at ambient temperatures displayed the characteristics of non-exchanging bidentate chelate complexes, sharp signals being detected for five ring and four ring-methyl hydrogens (Table 4). On warming solutions of the complexes exchange broadening occurred in all signals except that of the central pyridyl J hydrogen. Further warming led to band coalescences and subsequent sharpening to exchange-averaged signals. The fluxion could be followed by the pyrazole-ring proton exchange  $\text{B} \rightleftharpoons \text{E}$ , the pyridyl-hydrogen exchange  $\text{GHJ} \rightleftharpoons \text{HGJ}$  or the pyrazole-methyl exchanges  $\text{A} \rightleftharpoons \text{D}$  and  $\text{C} \rightleftharpoons \text{F}$ . In practice, the precise fitting procedure depended on the nature of the individual spectra. For the  $X = \text{Cl}$  complex both the pyridyl- and methyl-hydrogen signals were fitted for each temperature. For  $X = \text{Br}$  the pyridyl-hydrogen signals were chosen and for  $X = \text{I}$  the primary fitting was on the methyl signals and the chosen rate constants then further checked on the pyridyl G and H signals at each temperature.

The bandshape analysis for  $[\text{ReI}(\text{CO})_3(\text{tmbppy})]$  is shown in Fig. 6. In the static spectra the four methyl signals A, C, D and F are assigned as shown with the C and F signals exhibiting weak coupling ( $^4J = 0.7$  Hz) to the adjacent ring hydrogens. On warming, the exchanges  $\text{A} \rightleftharpoons \text{D}$  and  $\text{C} \rightleftharpoons \text{F}$  occurred with coalescences observed around 388 K ( $115^\circ\text{C}$ ). At the highest temperature measured (415 K) the spectra were approaching the fast-exchange limit, but the average C/F signal exhibited

**Table 7** Hydrogen-1 NMR data<sup>a</sup> for [ReBr(CO)<sub>3</sub>(dmbppy)] in the slow-exchange limit

Solvent	<i>T</i> /K	$\delta_{A/K}$	$\delta_{B/L}$	$\delta_{C/M}$	$\delta_{D/N}$	$\delta_{E/O}$	$\delta_{F/P}$	$\delta_{G/Q}$	$\delta_{H/R}$	$\delta_{J/S}$
CDCl <sub>3</sub>	273	8.19 (A)	6.80 (B)	8.34 (C)	2.34 (D)	6.17 (E)	2.38 (F)	7.78 (G)	7.32 (H)	8.19 (J)
		7.93 (K)	6.66 (L)	8.45 (M)	2.64 (N)	6.32 (O)	2.76 (P)	7.51 (Q)	7.70 (R)	8.16 (S)
CD <sub>2</sub> Cl <sub>2</sub>	263	8.17 (A)	6.80 (B)	8.40 (C)	2.28 (D)	6.15 (E)	2.30 (F)	7.82 (G)	7.33 (H)	8.23 (J)
		7.89 (K)	6.65 (L)	8.29 (M)	2.58 (N)	6.35 (O)	2.73 (P)	7.48 (Q)	7.73 (R)	8.18 (S)
$\Delta\delta^b$										
CDCl <sub>3</sub>	273	0.44 (A)	0.32 (B)	-0.10 (C)	0.03 (D)	0.13 (E)	-0.37 (F)	-0.04 (G)	-0.46 (H)	0.29 (J)
		0.18 (K)	0.18 (L)	0.01 (M)	0.33 (N)	0.28 (O)	0.01 (P)	-0.31 (Q)	-0.08 (R)	0.26 (S)
CD <sub>2</sub> Cl <sub>2</sub>	263	0.42 (A)	0.32 (B)	-0.04 (C)	-0.03 (D)	0.11 (E)	-0.45 (F)	0.00 (G)	-0.45 (H)	0.33 (J)
		0.14 (K)	0.17 (L)	-0.15 (M)	0.27 (N)	0.31 (O)	-0.02 (P)	-0.34 (Q)	-0.05 (R)	0.28 (S)
$^3J_{AB/LK}$ $^4J_{AC/KM}$ $^3J_{BC/LM}$ $^3J_{GJ/QS}$ $^3J_{HI/RS}$ $^4J_{DE/NO}$ $^4J_{DF/NP}$ $^4J_{EF/OP}$ $^4J_{GH/QP}$										
CDCl <sub>3</sub>	273	2.1	≈0	3.1	8.4	7.7	≈0	≈0	≈0.7	0.9
		1.7	≈0	2.6	8.0	8.1	≈0	≈0	≈0.7	0.9

<sup>a</sup> Relative to internal SiMe<sub>4</sub>,  $\delta$  0; scalar couplings  $J_{ij}$  in Hz. <sup>b</sup> Co-ordination shifts (*i.e.* relative to dmbppy).

**Table 8** Hydrogen-1 NMR shifts<sup>a</sup> of [ReBr(CO)<sub>2</sub>(tmbppy)] and co-ordination shifts of [ReBr(CO)<sub>3</sub>(tmbppy)] at 303 K in (CD<sub>3</sub>)<sub>2</sub>SO

	$\delta_A$	$\delta_B$	$\delta_C$	$\delta_D$	$\delta_E$	$\delta_F$	$\delta_G$	$\delta_H$	$\delta_J$
$\Delta\delta^b$	2.41	6.54	2.91	2.41	6.54	2.91	7.95	7.95	8.26
$\Delta\delta^c$	0.20	0.40	0.36	0.20	0.40	0.36	0.27	0.27	0.20
$\Delta\delta^d$	0.17	0.22	-0.02	0.17	0.22	-0.02	-0.22	-0.22	0.22
$\Delta\delta^e$	0.32	0.28	0.15	0.02	0.15	-0.19	0.05	-0.49	0.22

<sup>a</sup> Relative to internal SiMe<sub>4</sub>,  $\delta$  0. <sup>b</sup> Relative to tmbppy. <sup>c</sup> Co-ordination shifts for [ReBr(CO)<sub>3</sub>(tmbppy)] in the fast-exchange limit. Values based on averaged data at 303 K. <sup>d</sup> Co-ordination shifts for static [ReBr(CO)<sub>3</sub>(tmbppy)].

**Table 9** Activation energy data for 1,4-Re-N fluxions in [ReX(CO)<sub>3</sub>L] complexes

L	X	$\Delta H^\ddagger$ /kJ mol <sup>-1</sup>	$\Delta S^\ddagger$ /J K <sup>-1</sup> mol <sup>-1</sup>	$\Delta G^\ddagger$ /kJ mol <sup>-1</sup>	Ligand $pK_a^b$	Ref.
bppy	I	54.8 ± 0.8	-4 ± 3	56.0 ± 0.1	3.42	<i>c</i>
bppy	Br	50.8 ± 0.4	-18 ± 1	56.01 ± 0.04	3.42	<i>c</i>
bppy	Cl	53.4 ± 1.3	-7 ± 5	55.4 ± 0.1	3.42	<i>c</i>
dmbppy	Br	64.6 ± 1.6 <sup>d</sup>	-14 ± 5 <sup>d</sup>	68.7 ± 0.1 <sup>d</sup>	3.96	<i>c</i>
tmbppy	I	70.8 ± 1.0	-22 ± 3	77.3 ± 0.2	4.49	<i>c</i>
tmbppy	Br	68.5 ± 0.4	-15 ± 1	72.9 ± 0.1	4.49	<i>c</i>
tmbppy	Cl	70.1 ± 0.7	-1 ± 2	70.4 ± 0.1	4.49	<i>c</i>
terpy	I	76.3 ± 0.9	11 ± 2	73.0 ± 0.1	5.23	7
terpy	Br	79.8 ± 1.7	28 ± 5	71.6 ± 0.3	5.23	7
terpy	Cl	77.2 ± 1.4	23 ± 4	70.3 ± 0.2	5.23	7

<sup>a</sup> At 298.15 K. <sup>b</sup> Estimated from  $pK_a$  values of pyridine, pyrazole and 3,5-dimethylpyrazole. <sup>c</sup> This work. <sup>d</sup> Data refer to major → minor complex exchange.





**Fig. 5** Variable-temperature  $^1\text{H}$  NMR spectra of  $[\text{ReCl}(\text{CO})_3(\text{bppy})]$  in  $\text{CDCl}_3$ . See Table 3 for signal labelling. Signals marked **X** and  $\bullet$  are due to traces of  $\text{C}_6\text{D}_5\text{H}$  and  $\text{CHCl}_3$  respectively. Computer-synthesised spectra of the pyridyl hydrogens are shown on the left

some residual exchange broadening. Not all the experimental and computer-simulated spectra are shown in Fig. 6. Activation-energy data were calculated from eleven independent fittings in the temperature range shown and are listed for all three halide complexes in Table 9.

(iii)  $[\text{ReBr}(\text{CO})_3(\text{dmbppy})]$ . The fluxional process in this mixture of complexes became slow on the  $^1\text{H}$  NMR time-scale at *ca.*  $-10^\circ\text{C}$ . The assignment of the signals to the two chemically distinct complex species is given in Table 7. This assignment was based particularly on the two-dimensional COSY spectrum at  $-10^\circ\text{C}$  (Fig. 4) and the two-dimensional

EXSY spectrum at  $10^\circ\text{C}$  (Fig. 7), a temperature at which the fluxional process could be detected as cross-peak signals of all the ring hydrogens except J and S which had almost identical chemical shifts. The cross-peak signals confirmed the assignments and identified the hydrogen-pair exchanges  $\text{A} \rightleftharpoons \text{K}$ ,  $\text{B} \rightleftharpoons \text{L}$ ,  $\text{C} \rightleftharpoons \text{M}$ ,  $\text{E} \rightleftharpoons \text{O}$ ,  $\text{G} \rightleftharpoons \text{Q}$  and  $\text{H} \rightleftharpoons \text{R}$ . The methyl signals are not shown in this Figure but they also displayed the expected exchanges  $\text{D} \rightleftharpoons \text{N}$  and  $\text{F} \rightleftharpoons \text{P}$ .

A choice had to be made as to whether to use two-dimensional EXSY or one-dimensional bandshape analysis for measuring rates of the fluxional process. It was felt that the

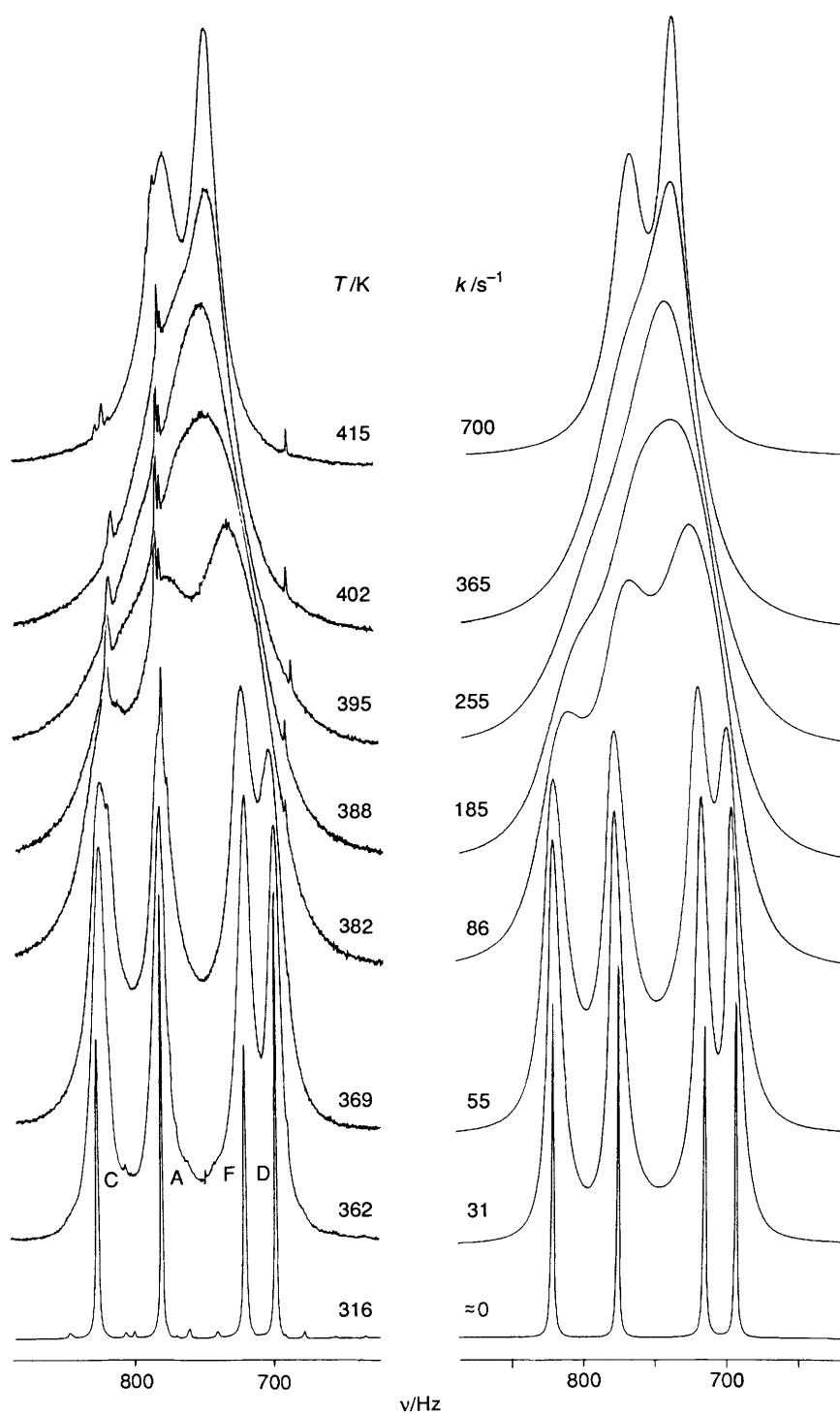


Fig. 6 Variable-temperature  $^1\text{H}$  NMR spectra of the methyl signals of  $[\text{ReI}(\text{CO})_3(\text{tmbppy})]$  in  $\text{CDCl}_2/\text{CDCl}_2$ . Computer-synthesised spectra with 'best-fit' rate constants are shown alongside

accuracy of the two-dimensional EXSY method might be affected by interference from COSY- and/or nuclear Overhauser enhancement spectroscopy (NOESY)-type cross-peaks, and the temperature range of study would be more restricted than that of bandshape analysis. The latter method was therefore chosen and spectra recorded in the range  $-10$  to  $140$   $^\circ\text{C}$  (Fig. 8). Fittings were actually carried out on the pyrazole hydrogen signals B, E, L and O in the temperature range  $10$ – $90$   $^\circ\text{C}$ , the populations of the two complexes being constant at  $75$  and  $25\%$  ( $\pm 1\%$ ) throughout this range. Activation-energy data based on these fittings are given in Table 9.

### Discussion

The 1,4-Re-N fluxion in these pyrazolylpyridine complexes occurs at distinctly different rates depending on the presence or absence of 3,5-dimethyl substitution on the pyrazole rings of the ligands (Table 9). Methyl substitution raises the energy barriers by  $15$ – $21$   $\text{kJ mol}^{-1}$ , such that in the tmbppy complexes the fluxion is slow on the  $^1\text{H}$  NMR time-scale at room temperature. In the bpy complexes, cooling to *ca.*  $-50$   $^\circ\text{C}$  is required effectively to 'freeze' the fluxion. Activation energies of the fluxion in the bpy complexes are essentially independent of halogen whereas in the tmbppy complexes a slight halogen dependence in  $\Delta G^\ddagger$  values

such that  $I > Br > Cl$  is observed. This may be a result of steric interactions of the pyrazole methyls with the halogen of the metal moiety. It is noteworthy that the same halogen dependence was detected in the corresponding terpy complexes<sup>7</sup> (Table 9), where the interaction involves the larger sized six-membered pyridyl rings. The activation energy for the fluxion of the dmbppy complex falls between those for bppy and tmbppy as expected, and the overall order of activation energies is  $bppy < dmbppy < tmbppy \approx terpy$ . This variation probably reflects the relative donor strengths of the N atoms in these heteroaromatic ligands and subsequent Re–N bond strengths. One measure of these donor properties would be the  $pK_a$  values of the ligands. These, however, are not known

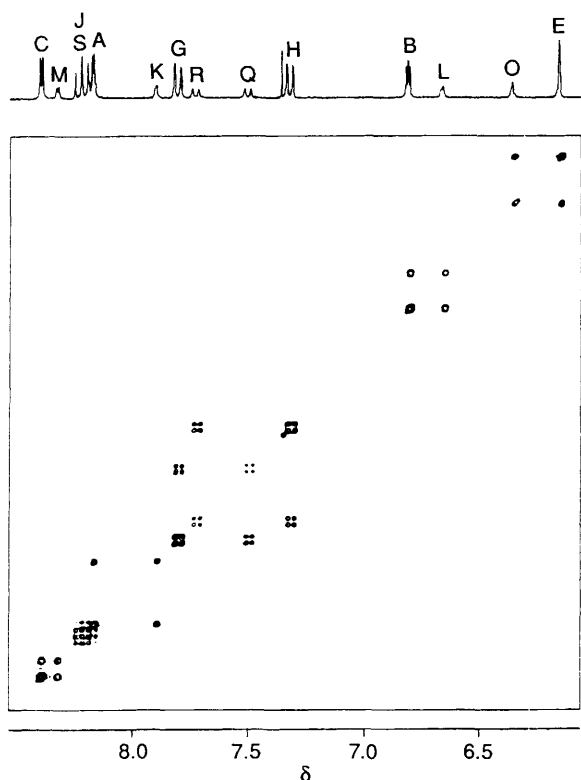


Fig. 7 The  $^1H$  two-dimensional EXSY spectrum of  $[ReBr(CO)_3-(dmbppy)]$  in  $CD_2Cl_2$  at  $-10\text{ }^\circ C$  showing the effects of the 1,4-fluxional shift. Mixing time was 0.5 s

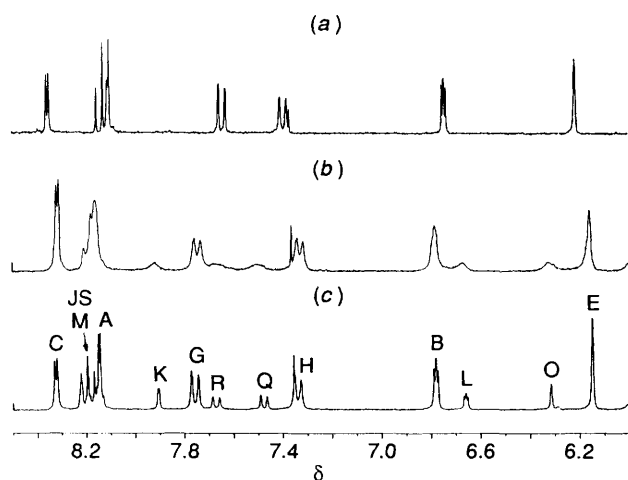


Fig. 8 Variable-temperature spectra of  $[ReBr(CO)_3-(dmbppy)]$  in  $CDCl_2/CDCl_2$  showing the effects of the 1,4-fluxional shift on the ring-hydrogen signals: (a) 140, (b) 30, (c)  $-10\text{ }^\circ C$

precisely but may be estimated from literature values for pyridine (5.23),<sup>20</sup> pyrazole (2.52)<sup>21</sup> and 3,5-dimethylpyrazole (4.12)<sup>21</sup> by the appropriate combination and averaging of these individual ring values. The resulting  $pK_a$  values given in Table 9 account roughly for the ordering of activation energies for the pyrazolylpyridine ligand complexes. However, the fluxional process in the terpy complex is predicted on the basis of ligand  $pK_a$  values to proceed more slowly with a somewhat higher activation energy than that actually measured. This discrepancy can be attributed to the different geometry of the terpy ligand with its three linked six-membered rings presenting a more favourable co-ordination geometry than that of one six- plus two five-membered rings of the pyrazolylpyridines. This difference may be quantified to a certain extent by considering the differences in the ligand bite angle for the free molecule and for the terdentate complex. From crystal-structure data for terpy and bppy the bite angles have been calculated<sup>14</sup> to be  $128$  and  $116^\circ$  respectively, whereas the corresponding angles for the terdentate complexes  $[RuL(PMe_3)_2(NO_2)]^+$  ( $L = terpy$  or  $bppy$ ) were  $158$  and  $157^\circ$  respectively. Thus greater structural changes are required in the bppy ligand when it goes from the free compound to the co-ordinated terdentate state. The same trend almost certainly exists in the present rhenium(i) complexes for the change from the bidentate ligand geometry to the quasi-terdentate geometry of the transition state of the fluxional process (see below). This therefore would account for the fluxional switching occurring more readily in the terpy complexes than predicted purely on the basis of the relative strengths of the Re–N bonds in both series of complexes.

The other question to be addressed is the mechanism of the fluxion. In the  $[PtXMe_3(terpy)]$  complexes<sup>8</sup> this was shown to involve a 'tick-tock' twist of the metal moiety through the N–Pt–N angle of the octahedral centre *via* a seven-co-ordinate platinum transition state in which all three N donors are weakly co-ordinated. This mechanism was confirmed by observation of

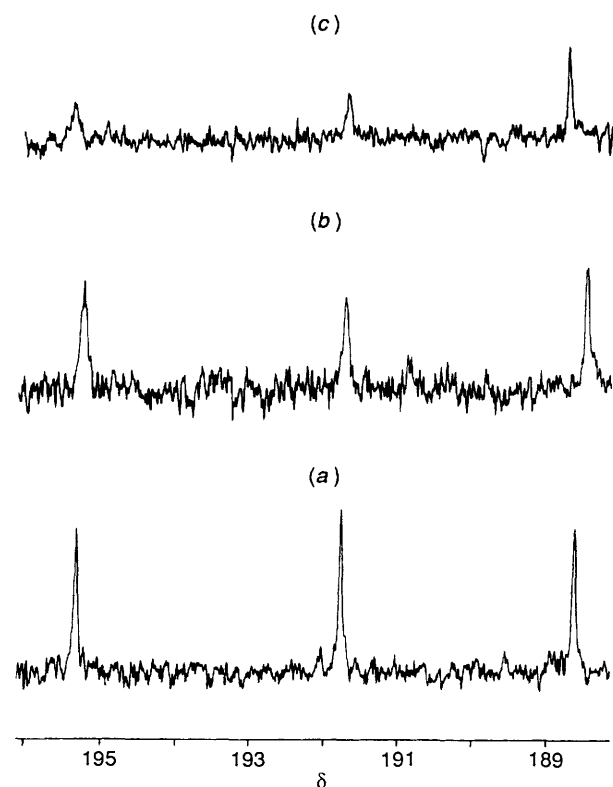
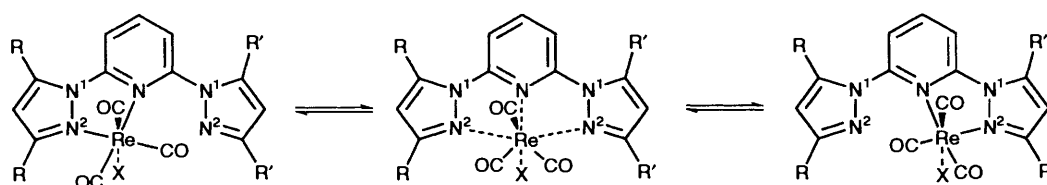


Fig. 9 The  $^{13}C$  NMR spectra (carbonyl region) of  $[ReI(CO)_3-(tmbppy)]$  in  $CDCl_2/CDCl_2$  at 30 (a), 60 (b) and 70  $^\circ C$  (c) showing exchange broadening of the equatorial carbonyl signals due to the fluxional shift



**Scheme 1** The 'tick-tock' twist mechanism of the fluxional process in the  $[\text{ReX}(\text{CO})_3\text{L}]$  ( $\text{L} = \text{bppy}$ ,  $\text{dmbppy}$  or  $\text{tmbppy}$ ) complexes

exchange of the two equatorial Pt–Me environments which necessarily results from this mechanism. In the case of the  $[\text{ReX}(\text{CO})_3(\text{terpy})]$  complexes<sup>7</sup> the same mechanism was inferred but not proven because of the difficulty in detecting the  $^{13}\text{C}$  NMR carbonyl signals. A more recent  $^{13}\text{C}$  NMR study of these complexes has, however, confirmed the existence of the 'tick-tock' mechanism in these complexes also.<sup>22</sup> In the present work the  $^{13}\text{C}$  NMR spectrum of  $[\text{ReI}(\text{CO})_3(\text{tmbppy})]$  was examined in detail with the aid of  $[\text{Cr}(\text{acac})_3]$  as a relaxation reagent (Tables 5 and 6). Spectra were recorded in  $\text{CDCl}_2/\text{CDCl}_2$  solvent at room temperature and at somewhat higher temperatures. Clear evidence of exchange broadening of two of the carbonyl signals (presumably the equatorial pair) was observed at 60 and 70 °C (Fig. 9) thereby confirming that the fluxion was again proceeding by the 'tick-tock' twist mechanism involving the breaking and making of two Re–N bonds (Scheme 1).

No evidence for restricted rotation of the unco-ordinated pyrazolyl rings was found in these rhenium complexes of  $\text{bppy}$  and  $\text{tmbppy}$ . This is in contrast to the restricted rotation observed in the corresponding  $\text{terpy}$  complexes.<sup>7</sup> Clearly, the smaller steric bulk of the five-membered pyrazolyl rings, even with methyl substituents, compared to the six-membered pyridyl rings enables rotations to be sufficiently free that rates are always fast on the NMR time-scale over the experimentally accessible temperature range.

This work has demonstrated the existence of a 1,4-M–N metalotropic shift in complexes of terpyridyl analogues as well as of terpyridine itself. The essential requirement for this fluxion appears to be an essentially planar chelate-ligand geometry with the ligand possessing at least one donor atom which is redundant to its bidentate chelate function.

#### Acknowledgements

We thank the University of Exeter for financial support for one of us (G. N. W.).

#### References

- 1 E. C. Constable, *Adv. Inorg. Chem. Radiochem.*, 1987, **30**, 69.
- 2 A. J. Canty, N. Chaichit, B. M. Gatehouse, E. George and G. Hayhurst, *Inorg. Chem.*, 1981, **20**, 2414.
- 3 G. B. Deacon, J. M. Patrick, B. W. Skelton, N. C. Thomas and A. H. White, *Aust. J. Chem.*, 1984, **37**, 929.
- 4 P. A. Anderson, F. R. Keene, E. Horn and E. R. T. Tiekink, *Appl. Organomet. Chem.*, 1990, **4**, 523.
- 5 E. W. Abel, N. J. Long, K. G. Orrell, A. G. Osborne, H. M. Pain and V. Šik, *J. Chem. Soc., Chem. Commun.*, 1992, 303.
- 6 E. R. Civitello, P. S. Dragovich, T. B. Karpishin, S. G. Novick, G. Bierach, J. F. O'Connell and T. D. Westmoreland, *Inorg. Chem.*, 1993, **32**, 237.
- 7 E. W. Abel, V. S. Dimitrov, N. J. Long, K. G. Orrell, A. G. Osborne, H. M. Pain, V. Šik, M. B. Hursthouse and M. A. Mazid, *J. Chem. Soc., Dalton Trans.*, 1993, 597.
- 8 E. W. Abel, V. S. Dimitrov, N. J. Long, K. G. Orrell, A. G. Osborne, V. Šik, M. B. Hursthouse and M. A. Mazid, *J. Chem. Soc., Dalton Trans.*, 1993, 291.
- 9 D. L. Jameson, J. K. Blaho, K. T. Kruger and K. A. Goldsby, *Inorg. Chem.*, 1989, **28**, 4312.
- 10 A. J. Downard, G. E. Honey and P. J. Steel, *Inorg. Chem.*, 1991, **30**, 3733.
- 11 S. Mahapatra, N. Gupta and R. N. Mukherjee, *J. Chem. Soc., Dalton Trans.*, 1991, 2911.
- 12 S. Mahapatra and R. N. Mukherjee, *J. Chem. Soc., Dalton Trans.*, 1992, 2337.
- 13 D. L. Jameson and K. A. Goldsby, *J. Org. Chem.*, 1990, **55**, 4992.
- 14 C. A. Bessel, R. F. See, D. L. Jameson, M. R. Churchill and K. J. Takeuchi, *J. Chem. Soc., Dalton Trans.*, 1992, 3223.
- 15 H. D. Kaesz, R. Bau, D. Hendrickson and J. M. Smith, *J. Am. Chem. Soc.*, 1967, **89**, 2844 and refs. therein.
- 16 M. M. Bhatti, Ph.D. Thesis, University of Exeter, 1980.
- 17 D. F. Shriver, *Manipulation of Air-sensitive Compounds*, McGraw-Hill, New York, 1969.
- 18 D. A. Kleier and G. Binsch, DNMR3, Program 165, Quantum Chemistry Program Exchange, Indiana University, IN, 1970.
- 19 H. Friebolin, *Basic One- and Two-dimensional NMR Spectroscopy*, 2nd edn., VCH, Weinheim, 1993, ch. 3.
- 20 J. Elguero, in *Comprehensive Heterocyclic Chemistry*, ed. K. T. Potts, Pergamon, Oxford, 1984, vol. 5, p. 223.
- 21 E. F. V. Scriven, in *Comprehensive Heterocyclic Chemistry*, eds. A. J. Boulton and A. McKillop, Pergamon, Oxford, 1984, vol. 2, p. 170.
- 22 H. M. Pain, unpublished work.

Received 15th November 1993; Paper 3/06799H